

# Antisense Intergenic Transcription Precedes *Igh* D-to-J Recombination and Is Controlled by the Intronic Enhancer $E_{\mu}^{\nabla\ddagger}$

Daniel J. Bolland,<sup>1</sup> Andrew L. Wood,<sup>1</sup> Rosh Afshar,<sup>2</sup> Karen Featherstone,<sup>1</sup>  
Eugene M. Oltz,<sup>2</sup> and Anne E. Corcoran<sup>1\*</sup>

Laboratory of Chromatin and Gene Expression, Babraham Institute, Babraham Research Campus,  
Cambridge CB22 3AT, United Kingdom,<sup>1</sup> and Department of Microbiology/Immunology,  
Vanderbilt University Medical School, Nashville, Tennessee 37232<sup>2</sup>

Received 22 December 2006/Returned for modification 2 February 2007/Accepted 16 May 2007

**V(D)J recombination is believed to be regulated by alterations in chromatin accessibility to the recombinase machinery, but the mechanisms responsible remain unclear. We previously proposed that antisense intergenic transcription, activated throughout the mouse *Igh*  $V_H$  region in pro-B cells, remodels chromatin for  $V_H$ -to-DJ<sub>H</sub> recombination. Using RNA fluorescence in situ hybridization, we now show that antisense intergenic transcription occurs throughout the *Igh*  $D_HJ_H$  region before D-to-J recombination, indicating that this is a widespread process in V(D)J recombination. Transcription initiates near the *Igh* intronic enhancer  $E_{\mu}$  and is abrogated in mice lacking this enhancer, indicating that  $E_{\mu}$  regulates  $D_H$  antisense transcription.  $E_{\mu}$  was recently demonstrated to regulate  $D_H$ -to- $J_H$  recombination of the *Igh* locus. Together, these data suggest that  $E_{\mu}$  controls  $D_H$ -to- $J_H$  recombination by activating this form of germ line *Igh* transcription, thus providing a long-range, processive mechanism by which  $E_{\mu}$  can regulate chromatin accessibility throughout the  $D_H$  region. In contrast,  $E_{\mu}$  deletion has no effect on  $V_H$  antisense intergenic transcription, which is rarely associated with  $D_H$  antisense transcription, suggesting differential regulation and separate roles for these processes at sequential stages of V(D)J recombination. These results support a directive role for antisense intergenic transcription in enabling access to the recombination machinery.**

In order to generate the primary repertoire of immunoglobulin (Ig) and T-cell receptor (TCR) molecules, antigen receptor loci undergo variable, diversity, and joining [V(D)J] recombination in B and T lymphocytes. Recombination is catalyzed by a recombinase complex containing the protein products of the recombinase-activating genes *Rag1* and *Rag2* (28). Within precursor lymphocytes, this process is strictly lineage specific, with heavy (*Igh*) and light (*Igk* and *Igl*) immunoglobulin loci fully recombining only in B lymphocytes and T-cell receptor loci (*Tcra*, *Tcrb*, *Tcrq*, and *Tcrd*) recombining only in T cells. Further, within lineages, loci are recombined in a precise order. Recombination of the *Igh* locus is the earliest step in the generation of the mature antibody repertoire in B lymphocytes. The *Igh* locus of the C57BL/6 mouse spans 3 Mb and comprises 195  $V_H$  genes spanning 2.5 Mb, 10  $D_H$  genes (~60 kb), 4  $J_H$  genes (2 kb), and 8 constant ( $C_H$ ) genes (200 kb) (31, 68).  $D_H$ -to- $J_H$  recombination occurs on both *Igh* alleles before  $V_H$ -to-DJ<sub>H</sub> recombination takes place (16).

Lineage and stage specificity of V(D)J recombination are regulated by differential chromatin accessibility to the RAG proteins. Several mechanisms may contribute, but their relative importance is still unclear. The first process discovered was germ line transcription, which occurs in all antigen receptor loci across gene segments competent for recombination (34).

This transcription was termed “sterile” or “germ line” to distinguish it from coding V(D)J transcription. In the *Igh* locus, the earliest germ line transcripts detected occur before  $D_H$ -to- $J_H$  recombination and initiate from two regions: the intronic enhancer  $E_{\mu}$  ( $I_{\mu}$  transcript) (35) and a promoter, PDQ52, immediately upstream of the most 3'  $D_H$  gene segment, DQ52 ( $_{\mu}0$  transcript) (60). Following  $D_H$ -to- $J_H$  recombination, the DJ<sub>H</sub> gene segment produces  $D_{\mu}$  transcripts (51) and sense germ line transcription initiates over the  $V_H$  genes (17, 67). The discovery of  $V_H$  gene germ line transcription formed the basis of the accessibility hypothesis, which proposed that lineage and stage specificity of recombination are regulated by differential chromatin accessibility of antigen receptor gene segments to the recombinase machinery, with germ line transcription associated with open chromatin (58, 67). However, a function for  $V_H$  germ line transcription has not been demonstrated, and it has been argued that it may be a secondary effect of the  $V_H$  gene promoters becoming accessible for  $V_H$ -to-DJ<sub>H</sub> recombination.

We have recently provided evidence in support of a functional role for germ line transcription with the discovery that an additional process, intergenic antisense transcription, not controlled by  $V_H$  gene promoters, occurs throughout the  $V_H$  region before  $V_H$ -to-DJ<sub>H</sub> recombination. We proposed that this large-scale transcription remodels the  $V_H$  region to facilitate accessibility for  $V_H$ -to-DJ<sub>H</sub> recombination (8).

Intergenic transcription has been proposed to drive through repressive chromatin, recruiting remodeling factors, thus facilitating further chromatin opening over genes (12). In several loci, intergenic transcription delineates domains of modified chromatin that surround active genes and their regulatory el-

\* Corresponding author. Mailing address: Laboratory of Chromatin and Gene Expression, Babraham Institute, Babraham Research Campus, Cambridge CB22 3AT, United Kingdom. Phone: 44 1223 496397. Fax: 44 1223 496022. E-mail: anne.corcoran@bbsrc.ac.uk.

‡ Supplemental material for this article may be found at <http://mc.manuscriptcentral.com/mcb>.

∇ Published ahead of print on 25 May 2007.

ements (7, 21, 25). RNA polymerase II is associated with, or recruits, a wide range of chromatin-remodeling and histone-modifying factors (14, 65, 66). Furthermore, transcription triggers histone turnover and the deposition of variant histone H3.3, enriched with active modifications (54). Collectively, these activities suggest several mechanisms by which the processing activity of the elongating RNA polymerase II complex can achieve chromatin accessibility (42, 47).

The process of intergenic transcription may therefore direct the changes in chromatin structure that precede V(D)J recombination. In the IgH V region, these include acetylation of histones H3 and H4, markers of accessible chromatin (15, 29, 38); histone H3.3 exchange (30); and methylation of H3 lysine 27 (H3-K27) (59). Indeed, it was recently demonstrated that disruption of intergenic transcription in the J $\alpha$  domain of the mouse TCR $\alpha$  locus results in failure both to methylate H3 lysine 4 and to recombine several corresponding J $\alpha$  genes (1), demonstrating a requirement for intergenic transcription to effect V(D)J recombination. In addition to localized changes, several large-scale changes in nuclear configuration occur, including repositioning of the *Igh* loci away from the nuclear periphery (32) and Pax-5-dependent contraction of the V<sub>H</sub> region, via higher-order looping of chromatin (23, 32, 53).

In the D region, increased DNase I sensitivity (15, 37), enrichment of acetylated histones H3 and H4, H3K4 methylation, and nucleosome remodeling over D<sub>H</sub> and J<sub>H</sub> genes occurs in pro-B cells poised for D<sub>H</sub>-to-J<sub>H</sub> recombination (15, 37, 43). Overall, while it is evident that several processes play critical roles in the regulation of V(D)J recombination, the precise role of each remains unclear.

It also remains to be clarified which regulatory elements direct V(D)J recombination of the *Igh* locus. It was originally proposed that the intronic enhancer E $_{\mu}$  regulated V<sub>H</sub>-to-DJ<sub>H</sub> recombination (52, 55). However, more recent studies by ourselves and others have shown that targeted deletion of E $_{\mu}$  causes a defect in D<sub>H</sub>-to-J<sub>H</sub> recombination, indicating that E $_{\mu}$  regulates this process primarily (2, 49). Thus, previously observed defects in V<sub>H</sub>-to-DJ<sub>H</sub> recombination are likely to be secondary to this earlier defect, and a V region-specific recombination control element has not yet been found. Although the function of E $_{\mu}$  in V(D)J recombination is now known, its mechanism of action remains unclear, and much remains to be understood about the chromatin regulation of the D<sub>H</sub> region before D<sub>H</sub>-to-J<sub>H</sub> recombination in vivo.

Our discovery of intergenic antisense transcription over the *Igh* V region before V-to-DJ recombination raised the question of whether similar transcriptional processes precede other V(D)J recombination events. Here we ask whether germ line transcription occurs over the D<sub>H</sub> region and whether this precedes and is functionally associated with D<sub>H</sub>-to-J<sub>H</sub> recombination.

#### MATERIALS AND METHODS

**Mice.** *Rag1*<sup>-/-</sup> mice (57), backcrossed to a C57BL/10 background, were kindly provided by M. Turner. C57BL/6 wild-type (WT) mice and timed matings were from the Small Animal Barrier Unit, Babraham Institute. PDQ52 and E $_{\mu}$  gene-targeted mice were as described previously (2). Animal work was performed under project license PPL 80/1644, in compliance with Home Office guidelines.

**Sorting of B-lymphocyte populations.** CD19<sup>+</sup> B lymphocytes from *Rag1*<sup>-/-</sup> bone marrow (BM) were sorted for RNA by positive selection using anti-CD19 magnetic affinity cell sorting (MACS) magnetic beads (Miltenyi Biotech; purity,

>80% CD19<sup>+</sup>). B220<sup>-</sup> interleukin 7R (IL-7R)<sup>+</sup> cells (common lymphoid progenitors [CLPs]) were fluorescence-activated cell sorter (FACS) sorted directly from WT BM without prior enrichment. We sorted B220<sup>+</sup>CD19<sup>+</sup> *Rag1*<sup>-/-</sup> BM B cells for RNA fluorescence in situ hybridization (RNA FISH) directly by FACS. The following antibodies, obtained from BD Pharmingen, were used: phycoerythrin-labeled, allophycocyanin (APC)-labeled, or biotinylated anti-B220 (RA3-6B2); fluorescein isothiocyanate (FITC)-, APC-, or peridinin chlorophyll-cy5.5-labeled or biotinylated anti-CD19 (1D3); and biotinylated anti-IL-7R (B12-1). The purity of each cell fraction was always >90%. Cells were washed twice in phosphate-buffered saline and then applied to poly-L-lysine-coated slides (Sigma) and fixed with 3.7% formaldehyde (Merck).

Fetal liver B cells were isolated by negative MACS selection using a biotinylated anti-Ter119 antibody (BD Pharmingen). B220<sup>+</sup>CD19<sup>+</sup> cells were then sorted from the negative fraction by FACS using the same antibodies described above. These cells were then used to make either RNA or slides for RNA FISH as described above. B220<sup>+</sup> cells were sorted from BM of *Rag*-deficient mice harboring either WT, PDQ52<sup>-/-</sup>E<sup>+/+</sup>, or P-E<sup>-</sup> alleles, using biotinylated anti-B220, followed by streptavidin-conjugated MACS beads.

**Reverse transcription-PCR analysis.** Total RNA was extracted from BM cell populations and cell lines using an RNeasy kit (QIAGEN) according to the manufacturer's protocol, except for total RNA from *Rag*-deficient mice harboring WT, PDQ52<sup>-/-</sup>E<sup>+/+</sup>, or P-E<sup>-</sup> alleles, which was isolated using TRIzol (Invitrogen Life Technologies). The RNA was treated with RNase-free DNase I (1 unit per  $\mu$ g of total RNA; Promega) for 1 h at 37°C followed by repurification using a QIAGEN RNeasy kit according to the manufacturer's RNA cleanup protocol. Between 0.1 and 0.5  $\mu$ g of total RNA was reverse transcribed for 2 h using Superscript III (Invitrogen) at either 50°C, with 100 ng of random hexamers (Amersham Pharmacia), or 55°C, with 2 pmol of specific reverse transcription primer (see Table S1 in the supplemental material). Reverse transcription reactions were assembled at 55°C to reduce endogenous priming. Following reverse transcription, PCR was performed with the primers listed in Table S1 in the supplemental material, using the following conditions: 30 to 40 cycles of 30 s at 94°C, 30 s at the annealing temperature, and 30 s at 72°C. Annealing temperatures varied according to the melting temperatures of the primer pairs (see Table S1 in the supplemental material). Inverted gel images were sufficient to visualize products, with the exception of 81X (see Fig. 3), which was detected by Southern blotting using a <sup>32</sup>P-labeled genomic DNA PCR product probe. DNA bands were excised, gel purified using a QIAquick gel extraction kit (QIAGEN), and cloned into the pGEM-T Easy vector (Promega) for sequencing. Real-time PCR was performed in triplicate on cDNA reverse transcribed with random hexamers as previously described, except 1  $\mu$ g of total RNA was used. PCRs were detected with SYBR green fluorogenic dye (Applied Biosystems) in an ABI PRISM 7000 sequence detection system (Applied Biosystems). Cycling conditions were as follows: 95°C for 10 min followed by 40 cycles of 95°C for 15 s and 60 to 64°C (depending upon primer pair) for 1 min. The PCR primers used are listed in Table S1 in the supplemental material. Relative quantification was performed after construction of standard curves using serial dilutions of genomic DNA, and values were then normalized to 3558.

**RNA FISH.** Sorted cells fixed on slides were analyzed by two-color RNA FISH essentially as described previously (24), with the modifications listed by Gribnau et al. (25). For three-color FISH, biotinylated probes were generated and detected with streptavidin Alexa 350 (Molecular Probes), followed by a biotinylated goat antistreptavidin antibody (Cambio), followed by an additional layer of streptavidin Alexa 350. When Alexa 350 was used, DAPI (4',6'-diamidino-2-phenylindole) was omitted from the mounting media. Probes for FISH were generated by PCR (primers are listed in Table S1 in the supplemental material), cloned into pGEM-T Easy vector (Promega), and verified by sequencing. Single-stranded cDNA probes for detection of either sense or antisense transcripts were generated by in vitro transcription using a MAXIscript kit (Ambion) followed by reverse transcription with Superscript II (Invitrogen) including either digoxigenic-11-dUTP (Roche), 2,4-dinitrophenol-11-dUTP (Perkin Elmer), or biotin-11-dUTP (Roche) in the reaction (11). In hybridizations, antisense probes detected complementary sense transcripts, while sense probes detected antisense transcripts. Signals were visualized and captured using Olympus BX40 and BX41 microscopes. Experiments were performed two to three times, and at least 100 nuclei (two colors) or 100 alleles (three colors) were counted each time. Total numbers of cells counted are shown in Table S2 in the supplemental material.

#### RESULTS

**Germ line antisense and intergenic transcription occurs throughout the D<sub>H</sub> region.** We assembled in silico the entire

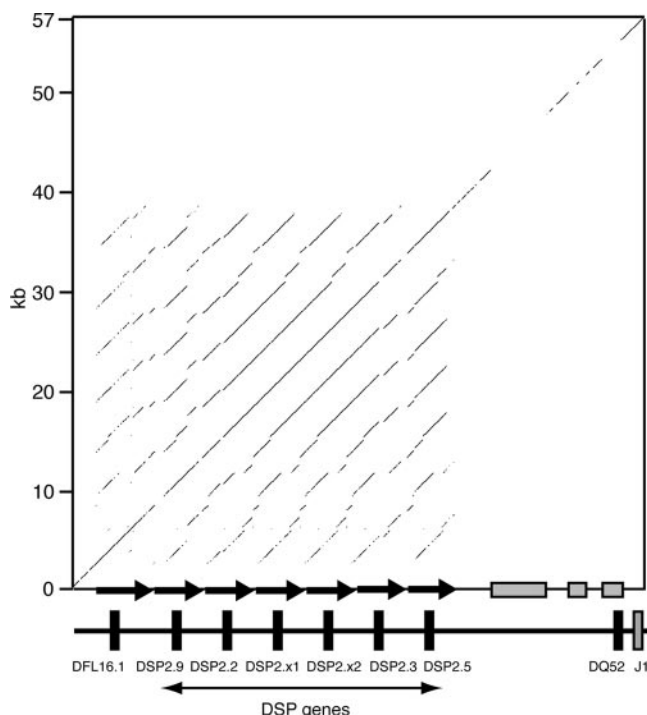


FIG. 1. DFL and DSP genes are located in a tandem array of ~4.7-kb repeats. The sequence of the  $D_H$  region of C57BL/6 was aligned against itself using the DotPlot program from the Omega package (Accelrys). The interspersed repeats within the sequence on the vertical axis were masked with X's using RepeatMasker ([www.repeatmasker.org](http://www.repeatmasker.org)) to exclude these from the alignment, resulting in a discontinuous diagonal line, in particular in the DSP2.5-DQ52 intergenic region, which contains several interspersed repeats (gray boxes on x axis). Black arrows depict the ~4.7-kb direct repeats containing the DSP and DFL16.1 genes. A sliding window of 30 bp was used; lines indicate  $\geq 90\%$  identity.  $D_H$  genes are labeled in accordance with Ye (68). For clarity, the DST4 and P2-P6 genes are not depicted.

$D_H$  region of the C57BL/6 mouse *Igh* locus from available genomic sequences. Subsequently, the assembly of this region was reported elsewhere (68). Within this sequence, all  $D_H$  gene segments are oriented in the same (sense) direction relative to the constant region genes. The C57BL/6  $D_H$  region is organized as a tandem array of seven 4.7-kb repeats, each repeat containing a DFL16.1 or DSP gene (Fig. 1). The DSP repeats are almost identical to each other (95 to 99%), while the DFL16.1 repeat is ~85% identical to each of the DSP repeats. The most 3' D gene, DQ52, is separated from the DFL/DSP tandem array by ~20 kb of unique sequence and has very different flanking sequences, including the PDQ52 promoter/enhancer (33).

We first investigated germ line transcription of the DFL16.1/DSP region, since this constitutes most of the  $D_H$  region and the vast majority of  $D_H$  gene usage in V(D)J recombination in C57BL/6 mice (20, 68). We designed reverse transcription and nested PCR primers to detect all the DSP genes equally in a single reaction and a set to detect the DFL16.1 gene separately. Reverse transcription and PCR primers were located downstream of the  $D_H$  gene 3' recombination signal sequence (RSS) (Fig. 2A). As the 3' RSS is lost due to  $D_H$ -to- $J_H$  recombination, only transcripts originating from unrearranged  $D_H$

segments will be detected in WT mice. We first analyzed ex vivo CD19<sup>+</sup> BM cells from *Rag1*<sup>-/-</sup> mice (57) using a sensitive strand-specific reverse transcription-PCR assay (8). As these mice cannot perform V(D)J recombination, any  $D_H$  transcripts detected would be exclusively germ line in origin.

We reverse transcribed total RNA from *Rag1*<sup>-/-</sup> CD19<sup>+</sup> BM cells using random hexamers or gene-specific primers and performed PCR on the cDNA using nested primers. In both random and antisense-specific reverse transcription-PCRs, cDNA products of the same size as those from genomic DNA were amplified for both DSP and DFL, while no sense-specific products were amplified (Fig. 2C, i and ii). We did not detect any sense  $D_H$  germ line transcription using two further sets of reverse transcription and nested PCR primers, confirming previous findings (3). However, as previously described (8), we detected sense, but not antisense, transcription over the  $I_\mu$  intron and  $C_\mu$  exons 2 to 3 (Fig. 2B and C). We conclude that antisense, but not sense, transcription occurs over the germ line D genes of the *Igh* locus.

We next determined whether  $D_H$  antisense transcription was exclusively associated with the genes or extended into intergenic regions. As the intergenic sequences between the DSP genes are 95 to 99% identical, we were able to design one set of nested primers that would amplify interspersed repeat-free regions between each of the six DSP genes with equal efficiency (Fig. 2B, iii). Strand-specific reverse transcription-PCR showed an unspliced antisense band of the expected size, indicating that antisense transcription also occurred in intergenic regions (Fig. 2C, iii). We cloned and sequenced both the genic and intergenic reverse transcription-PCR products to find out whether the whole DSP array was transcribed or if the observed transcription was occurring across only certain regions. All but one DSP gene and one intergenic region were represented, indicating that transcription occurs across the entire DSP region (Fig. 2D).

We next investigated if the antisense transcription extended outside the DFL/DSP array using reverse transcription and nested PCR primers located between the most 3' DSP gene, DSP2.5, and the most J-proximal D gene, DQ52 (Fig. 2B, iv). A strong antisense-specific band, but no sense band, was detected, indicating that the DSP-DQ52 intergenic region was also transcribed in the antisense orientation (Fig. 2C, iv). Taken together, the data indicate that antisense intergenic transcription extends throughout the  $D_H$  region.

To gain insight into how abundant these transcripts are and how their amounts compared to antisense transcripts we have previously detected in the V region, we performed quantitative real-time reverse transcription-PCR. We compared transcription from the unique DF16 gene with two unique intergenic regions, the first within the J558 gene family which comprises the 5' half of the V region and the second from the J606 family in the middle of the V region. The reverse transcription reaction was performed with random hexamers so that the subsequent PCRs could be performed on the same sample. In all three cases, transcription has previously been detected only from the antisense strand. DFL16 transcript amounts were intermediate between J558 and J606, and variation was no greater than 2.5-fold among all three regions (Fig. 2E), indicating that steady-state amounts of antisense transcription over the D region are comparable to the V region in *Rag1*<sup>-/-</sup>

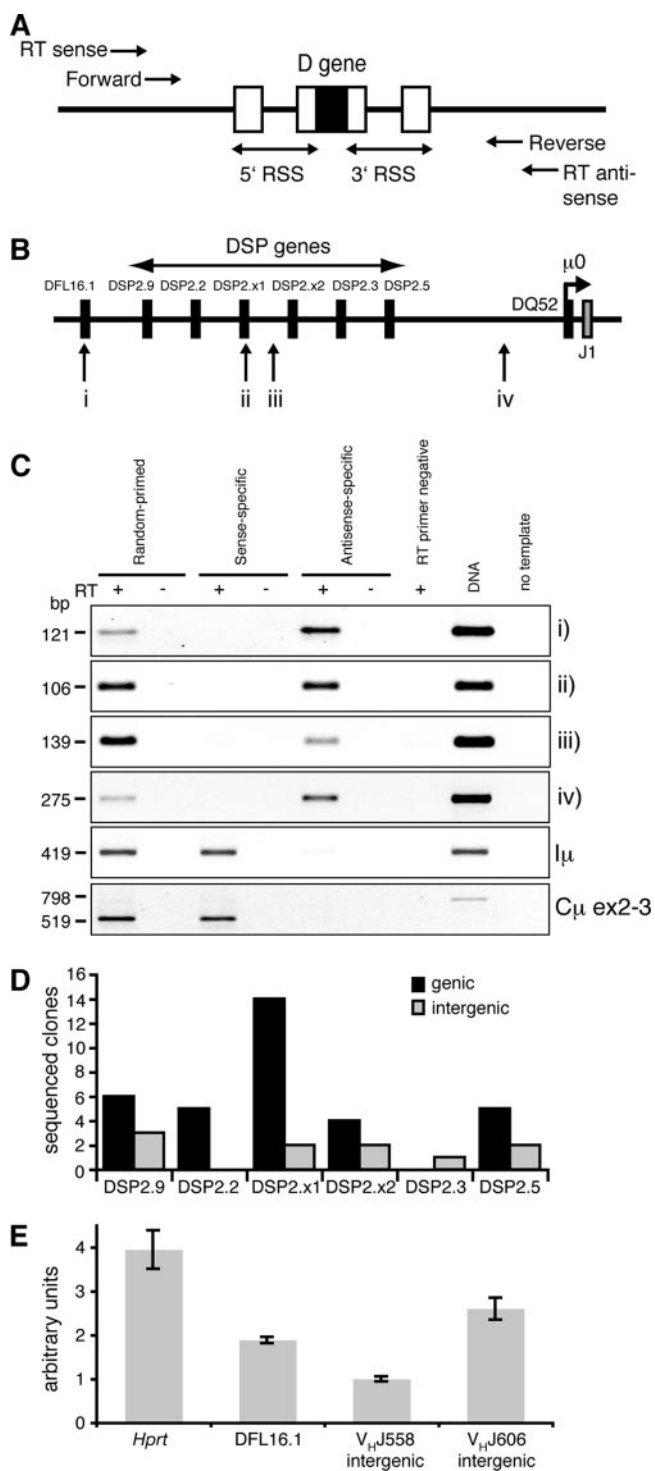


FIG. 2. Detection of germ line transcription across the *Igh* D region. (A) Design of the  $D_H$  region germ line transcription reverse transcription-PCR assay. Reverse transcription antisense (to detect sense transcription) and sense (to detect antisense transcription) primers were designed 5' and 3' of the  $D_H$  gene RSS sequences. Nested primers were used for PCR. Similar schemes were used for intergenic regions. (B) Schematic of the DFL16.1-J1 sequence showing regions analyzed by reverse transcription-PCR. Not to scale. (C) Reverse transcription-PCR of *Rag1*<sup>-/-</sup> CD19<sup>+</sup> total RNA. Above lanes, with (+) or without (-) reverse transcriptase (RT). Right margin, regions amplified (shown in panel B); left margin, molecular sizes. DNA, genomic

CD19<sup>+</sup> BM cells. Furthermore, amounts were within fourfold of the housekeeping gene, hypoxanthine-guanine phosphoribosyltransferase (HPRT), indicating that these transcripts are relatively abundant.

#### Developmental regulation of $D_H$ antisense transcription.

We next sought to investigate the stage specificity of  $D_H$  antisense transcription during B-lymphocyte development and V(D)J recombination. B lymphopoiesis initiates in the fetal liver with B-cell progenitors appearing by day 12.5 (18).  $D_H$ -to- $J_H$  recombination initiates on day 12 and increases rapidly on days 13 and 14 (19). Thus, fetal liver on day 14 and day 15 includes B cells that have initiated and those that have completed  $D_H$ -to- $J_H$  recombination (26). Consequently, initiation of  $V_H$ -to- $DJ_H$  recombination is similarly asynchronous, and this is reflected by the reported expression of  $V_H$  germ line sense gene transcripts from day 14 until day 16 (36). Thus, in fetal liver,  $D_H$ -to- $J_H$  recombination and  $V_H$ -to- $DJ_H$  recombination occur in partially overlapping temporal windows.

We first investigated steady-state transcript levels in BM progenitor B lymphocytes from *Rag1*<sup>-/-</sup> (CD19<sup>+</sup>) and day 14.5, 15.5, and 16.5 WT fetal liver B cells. Further, to obtain a more detailed picture of when  $D_H$  antisense transcription initiates, we also examined BM CLPs (IL-7R<sup>+</sup> B220<sup>-</sup>), which undergo a low level of  $D_H$ -to- $J_H$  recombination (4). We analyzed thymus to study the association of  $D_H$  antisense transcription specifically with  $D_H$ -to- $J_H$  recombination, since up to 50% of thymocytes undergo  $D_H$ -to- $J_H$  but are blocked from completing  $V_H$ -to- $DJ_H$  recombination (9). We used brain as a negative control. By semiquantitative reverse transcription-PCR, we first analyzed expression of V region germ line transcripts. Random-primed reverse transcription followed by PCR to detect the largest J558 gene family in the D-distal end of the V region yielded two transcript bands, as previously shown for BM early B cells. The lower band corresponds to the spliced sense transcript, while the upper band includes both antisense and unspliced sense primary transcripts (8). Both bands were present in fetal liver B cells, with little variation between days 14.5 and 16.5 (Fig. 3), confirming previous Northern analysis (36). We found a similar developmental distribution of germ line transcripts from the D-proximal 7183 V gene family, albeit transcript levels were lower, due in part to PCR detection of fewer genes (Fig. 3). Neither transcript was present in the thymus, consistent with the V region's being inaccessible in thymocytes (Fig. 3). Steady-state  $D_H$  antisense transcription levels were similar to those in *Rag1*<sup>-/-</sup> CD19<sup>+</sup> cells in fetal liver B-cell populations, with little change between days 14.5, 15.5, and 16.5 (Fig. 3).  $D_H$  antisense transcripts are absent from brain (not shown) and low in CLPs but are readily detectable in thymocytes (Fig. 3). Taken together, these results

DNA positive control. (D) Sequencing of DSP genic and intergenic reverse transcription-PCR products. The number of reverse transcription-PCR products cloned and sequenced is shown for each  $D_H$  gene and intergenic region. (E) Real-time quantitative reverse transcription-PCR of *Rag1*<sup>-/-</sup> CD19<sup>+</sup> random-primed cDNA showing relative transcription levels for *Hprt*, DFL16.1, *V<sub>H</sub>J558* intergenic, and *V<sub>H</sub>J606* intergenic regions. The level of *V<sub>H</sub>J558* intergenic transcription was arbitrarily set to 1.

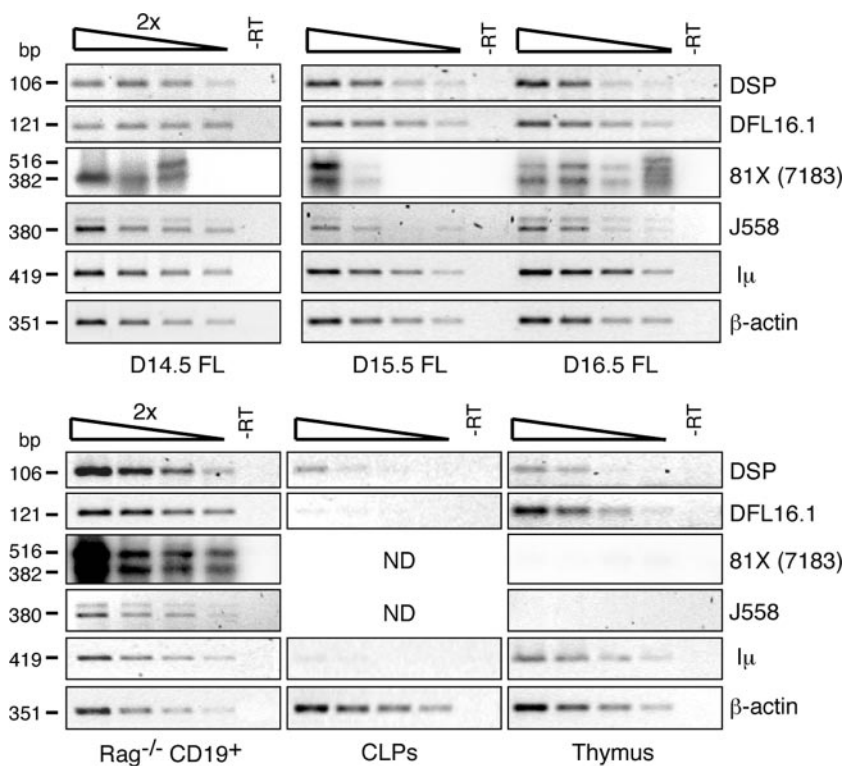


FIG. 3. Semiquantitative reverse transcription-PCR analysis of  $D_H$  antisense and  $V_H$  genic germ line transcription through development. Top panel: Day (D)14.5, D15.5, and D16.5 fetal liver B lymphocytes. Bottom panel:  $Rag1^{-/-}$   $CD19^+$  BM B lymphocytes, CLPs, and ex vivo thymocytes. Right margin, regions amplified; left margin, molecular sizes. -RT, without reverse transcriptase.  $\beta$ -actin was used as a loading control. DSP and DFL16.1 antisense transcripts were detected as in Fig. 2. 81X and J558 were amplified by random-primed reverse transcription-PCR. The PCR primers were designed to amplify one (81X) or nine (J558) V genes. 81X products were subjected to blotting Southern and probed with a genomic DNA PCR product to aid visualization.

suggest that  $D_H$  antisense transcription initiates on *Igh* alleles poised for  $D_H$ -to- $J_H$  recombination.

Reverse transcription-PCR was used to assess steady-state transcript levels in bulk populations. However, we sought to analyze  $D_H$  antisense primary transcription on individual *Igh* alleles in single cells to determine its association with the different steps of V(D)J recombination of the locus and thus provide clues to its function. To do this, we used RNA FISH. We designed 3.5-kb DFL16.1 and 2.8-kb DSP2.x1 RNA FISH probes containing each gene and respective flanking region (Fig. 4A). As the DSP repeats are >95% identical, it is likely that the DSP2.x1 probe detects transcription of all DSP genes. As the DFL and DSP segments are highly homologous, it was also probable that the probes would cross-hybridize. Therefore, for optimal detection efficiency, we combined the probes in all cases.

To first determine if we could detect D antisense intergenic transcription by RNA FISH, we analyzed  $CD19^+$  pro-B cells from  $Rag1^{-/-}$  mice. Sense or antisense  $D_H$  probes were cohybridized with a probe for  $I_\mu$ , described previously (8). We used  $I_\mu$  as a positive control, as it is transcribed from a high proportion of alleles (8) (Fig. 4A). We detected  $D_H$  antisense signals in 37% of  $Rag1^{-/-}$   $CD19^+$  pro-B cells with  $I_\mu$  signals. We did not detect any  $D_H$  sense signals, in agreement with the reverse transcription-PCR results.  $D_H$  antisense signals were closely associated with or overlapping the  $I_\mu$  signals, as ex-

pected, given that the DSP/DFL region is located just ~24 kb from  $E_\mu$  (Fig. 4B). We detected biallelic  $D_H$  antisense transcription in ~10% of cells, indicative of the stochastic output of a biallelically expressed transcription unit transcribing at a low level (61). In conclusion, we were able to detect  $D_H$  antisense transcription by RNA FISH in a high proportion of  $Rag1^{-/-}$  pro-B cells.

We next investigated  $D_H$  antisense intergenic transcription in day 14.5, 15.5, 16.5, and 17.5 fetal liver  $B220^+CD19^+$  B-lymphocyte populations (Fig. 4C).  $I_\mu$  signals were detected in approximately 60% of cells in each of these samples, indicating that a large proportion of *Igh* alleles are active in fetal liver B lymphocytes. In day 14.5 and 15.5 populations, we detected  $D_H$  antisense signals in comparably high proportions of cells (30% and 32% of cells with  $I_\mu$  signals, respectively). By day 16.5, the number of B cells with  $D_H$  antisense signals was reduced to ~18%, and this number was further reduced to 7% by day 17.5 (Fig. 4F). Thus,  $D_H$  antisense transcription occurs over an extended time window during fetal liver B-lymphocyte development but is progressively lost, probably as a result of ongoing V(D)J recombination (see below).

To further clarify how  $D_H$  antisense transcription relates to V(D)J recombination in fetal liver, we analyzed the appearance of sense transcripts from VDJ $_H$ -rearranged alleles.  $V_H$  sense germ line transcripts are undetectable by our RNA FISH technique (8); thus, all  $V_H$  sense transcription signals detected

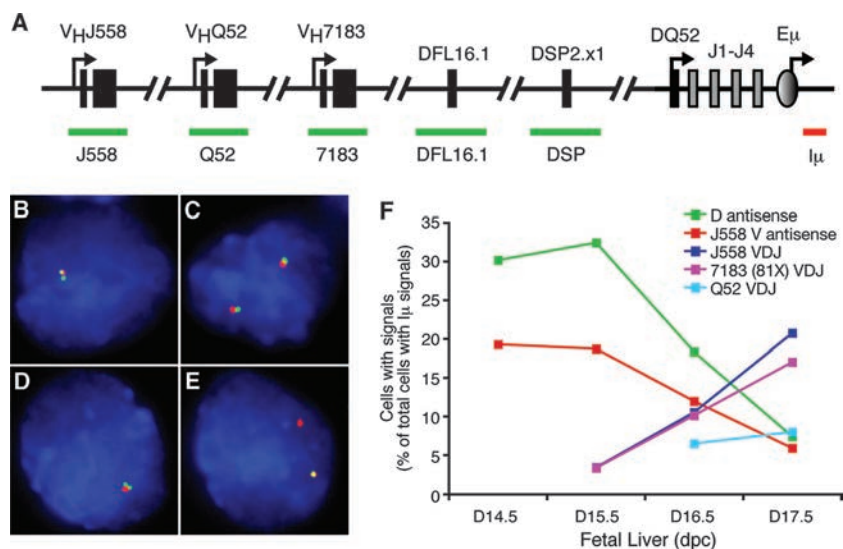


FIG. 4. Developmental regulation of  $D_H$  antisense transcription in fetal liver B lymphocytes. (A) Locations of RNA FISH probes: red, detected with Texas Red; green, detected with FITC. RNA FISH detection of  $D_H$  antisense intergenic and  $I_\mu$  sense transcription in (B)  $CD19^+$   $Rag1^{-/-}$  BM and (C) WT E15.5 fetal liver B lymphocytes. (D) RNA FISH detection of  $V_HJ558$  antisense transcription in day 15.5 fetal liver B lymphocytes. (E) RNA FISH detection of  $V_HJ558$  VDJ-rearranged (VDJ $_H$ ) transcription in day (D)16.5 fetal liver B lymphocytes. Similar signals were obtained for  $V_H7183$  and  $V_HQ52$ . In all cases, nuclei were counterstained with DAPI (blue). (F) Quantitation of  $D_H$  antisense,  $V_HJ558$  antisense,  $J558$  VDJ $_H$ ,  $7183$  (81X) VDJ $_H$ , and  $Q52$  VDJ $_H$  RNA FISH signals in  $CD19^+$  B lymphocytes from D14.5, D15.5, D16.5, and D17.5 fetal liver.

originate from VDJ $_H$ -rearranged alleles. We used probes to detect VDJ $_H$ -rearranged transcription for the 3'  $V_H7183$  (81X) and  $V_HQ52$  families and the large 5'  $V_HJ558$  family (8). In day 15.5 fetal liver B lymphocytes, we detected VDJ $_H$  signals for both  $V_H7183$  and  $V_HJ558$  in similarly low numbers of cells (~3% of cells with  $I_\mu$ ) (Fig. 4E and F). By day 16.5, signals for both families had increased to 10%, while at day 17.5,  $V_H7183$  signals were found in 17% and  $V_HJ558$  signals in 21% of cells with  $I_\mu$  signals. This distribution is as expected, given the greater number of  $J558$  genes (31), tempered by a mild bias toward  $V_H7183$  recombination in C57BL/6 fetal liver (5). These results correlated well with a previous report of Northern blot detection of  $J558$  VDJ $_H$  transcripts from day 16.5 of development (36). Signals from the  $V_HQ52$  family were found in 6.5% and 8% of day 16.5 and 17.5 B lymphocytes, respectively (Fig. 4F). Thus,  $V_H$ -to-DJ $_H$  recombination also occurs asynchronously over an extended temporal window. Together, these findings show that by the time VDJ $_H$  signals are seen in appreciable numbers (day 16.5), the number of  $D_H$  antisense signals is greatly reduced, consistent with  $D_H$  antisense transcription's being lost as a result of ongoing V(D)J recombination.

Due to the overlapping time windows of  $D_H$ -to- $J_H$  and  $V_H$ -to-DJ $_H$  recombination, we had not yet determined the extent to which  $D_H$  antisense intergenic transcription was associated with each of these processes. To place it in context relative to the accessibility of the  $V_H$  region, we next analyzed  $V_H$  antisense transcription in fetal liver. Using a probe to the  $V_HJ558$  antisense transcripts from the 5' half of the V region (8), we discovered that  $V_H$  region antisense transcription is present in a relatively high number of cells by day 14.5 (19% of cells with  $I_\mu$  signals) (Fig. 4D and F). This proportion remains similar on day 15.5 (18.5%) but is reduced by day 16.5 (12%) and further reduced by day 17.5 (6%). Thus,  $V_H$  and  $D_H$  antisense tran-

scription processes also overlap significantly within the same time window, albeit transcripts may occur on different alleles or indeed in different cells.

The sharp reduction in both D and V antisense primary transcripts between day 15.5 and day 16.5 and thereafter (Fig. 4F) contrasted with steady-state transcript levels, which showed little variation between days 14.5 and 16.5 (Fig. 3). RNA FISH detects a window of primary transcript generation and thus is exquisitely dependent on the presence of an actively transcribing locus and appropriate target sequence, which is lost due to ongoing V(D)J recombination. In contrast, steady-state levels reflect the balance between generation and degradation of transcripts, and the relatively stable levels observed suggest low transcript turnover.

**$D_H$  antisense transcription initiates on germ line alleles and before  $V_H$  antisense transcription.** To distinguish between these possibilities, we first determined if  $D_H$  and  $V_H$  antisense transcription occurred on germ line alleles in day 15.5 fetal liver B lymphocytes using three-color RNA FISH. We cohybridized probes to detect  $I_\mu$ ,  $\mu_0$ , and either  $D_H$  (DSP and DFL) or  $V_H$  ( $J558$ ) antisense transcription (Fig. 5A). The  $\mu_0$  probe is located between DQ52 and J1; since this region is removed by  $D_H$ -to- $J_H$  recombination, this probe is a marker of unrearranged alleles. We detected  $I_\mu$  in blue,  $\mu_0$  in red, and  $D_H$  or  $V_H$  antisense transcription in green. We found that  $D_H$  antisense signals colocalized with  $\mu_0$  and  $I_\mu$  in 36% of total alleles counted in day 15.5 fetal liver B lymphocytes, while  $D_H$  antisense signals occurred without  $\mu_0$  on 17% of total alleles (Fig. 5A and C). Thus, 70% of  $D_H$  antisense transcripts were associated with  $\mu_0$ , indicating that  $D_H$  antisense transcription initiates on germ line alleles in fetal liver. A total of 30% of alleles expressed  $D_H$  antisense transcripts without  $\mu_0$ , suggesting that  $D_H$  antisense transcription continues on DJ $_H$ -rearranged alleles.

In contrast,  $V_H$  antisense,  $\mu_0$ , and  $I_\mu$  colocalized in only 9%

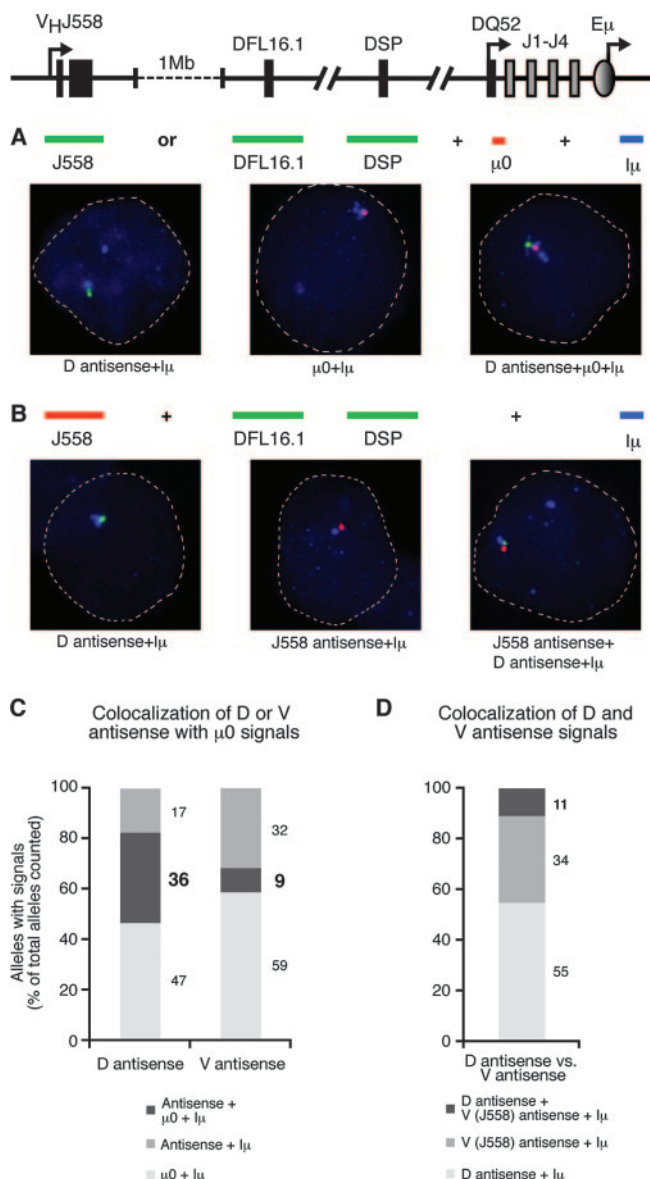


FIG. 5. Analysis of colocalization of  $D_H$  and  $V_H$  antisense signals with  $\mu_0$  and with each other. (A) Locations of RNA FISH probes: red, detected with Texas Red; green, detected with FITC; blue, detected with Alexa 350. Three-color RNA FISH detection of  $D_H$  antisense or  $V_H$  antisense,  $\mu_0$ , and  $I_{\mu}$  transcription. (B) Locations of RNA FISH probes: red, detected with Texas Red; green, detected with FITC; blue, detected with Alexa 350. Three-color RNA FISH detection of  $D_H$  antisense,  $V_H$  antisense, and  $I_{\mu}$  sense transcription. All experiments were performed with day (D)15.5 fetal liver B lymphocytes; representative examples of the different signals observed are given in each case. (C) Analysis of colocalization frequencies of  $D_H$  antisense or  $V_H$  antisense with  $\mu_0$  and  $I_{\mu}$ . (D) Analysis of colocalization frequencies of  $D_H$  antisense,  $V_H$  antisense, and  $I_{\mu}$ .

of total alleles, while  $V_H$  antisense transcripts were detected without  $\mu_0$  on 32% of total alleles (Fig. 5C). Thus, only 20% of  $V_H$  antisense signals were associated with  $\mu_0$ . Together, these results suggest that  $D_H$  antisense transcription precedes  $D_H$ -to- $J_H$  recombination of the *Igh* locus in fetal liver, and that  $V_H$  antisense transcription can initiate before  $D_H$ -to- $J_H$  recombi-

nation on a small number of alleles, but usually occurs concomitant with or following  $D_H$ -to- $J_H$  recombination, as previously shown in BM (8).

Given the differing associations with germ line alleles, we hypothesized that  $D_H$  and  $V_H$  antisense transcription would rarely be found on the same allele. To test this, we cohybridized probes to  $I_{\mu}$ ,  $D_H$  (DSP and DFL), and  $V_H$  (J558) antisense transcripts in day 15.5 fetal liver B lymphocytes (Fig. 5B). We detected  $I_{\mu}$  in blue,  $D_H$  antisense in green, and  $V_H$  antisense in red (Fig. 5B). We found that  $D_H$  and  $V_H$  antisense signals colocalized in 11% of alleles (Fig. 5D). Thus, while  $D_H$  and  $V_H$  antisense transcription can occur simultaneously on a low number of alleles, the majority (89%; 55%  $D_H$ , 34%  $V_H$ ) occurs separately. These data demonstrate a developmental shift from  $D_H$  antisense transcription to  $V_H$  antisense transcription concomitant with  $D_H$ -to- $J_H$  recombination in fetal liver.

**The *Igh* intronic enhancer  $E_{\mu}$  regulates  $D$  antisense intergenic transcription.** The data thus far provided strong correlative evidence in support of a role for  $D_H$  antisense intergenic transcription in chromatin accessibility for  $D_H$ -to- $J_H$  recombination. To test this model functionally, we assessed the role of the known regulatory elements PDQ52 and the intronic enhancer  $E_{\mu}$  in regulating  $D_H$  antisense transcription.

The PDQ52 promoter region initiates  $\mu_0$  transcription in the sense direction through the J-C $\mu$  region and is also thought to have enhancer function (33). We first asked if, similar to one other immunoglobulin promoter (45), PDQ52 was bidirectional and thus also the promoter of the  $D_H$  antisense transcription. To test this, we designed reverse transcription and nested PCR primers to amplify regions upstream and downstream of PDQ52 and did reverse transcription-PCR on CD19<sup>+</sup> *Rag1*<sup>-/-</sup> BM RNA (Fig. 6). Antisense-specific products of similar band intensities were amplified for both of these regions, indicating that antisense transcription occurs both upstream and downstream of PDQ52 and, hence, PDQ52 is unlikely to be the promoter of, or to regulate, the antisense transcription. This suggested that the downstream enhancer  $E_{\mu}$  might regulate  $D_H$  antisense transcription. This was an attractive hypothesis, as we had previously shown that  $E_{\mu}$  was required for D-to-J recombination (2).

To investigate this hypothesis, we analyzed  $D_H$  antisense transcription in two gene-targeted mouse models we have previously generated (2). The first contains a 300-bp deletion of the region upstream of DQ52 containing the  $\mu_0$  promoter PDQ52 and has no effect on V(D)J recombination of the *Igh* locus. The second contains a deletion of both PDQ52 and a 700-bp region spanning the core  $E_{\mu}$  and its 5' matrix attachment region (MAR). These mice have a dramatic defect in  $D_H$ -to- $J_H$  recombination, which, in the absence of a phenotype with the PDQ52 deletion alone, indicates that this process is regulated by  $E_{\mu}$  alone (2, 49).

We examined  $D_H$  region sense and antisense transcription by reverse transcription-PCR in B220<sup>+</sup> BM B lymphocytes from mice harboring these deletions on a *Rag*-deficient background, which ensured no interference from DJ<sub>H</sub>- or VDJ<sub>H</sub>-rearranged transcripts.  $D_H$  antisense transcripts were detected in PDQ52<sup>-/-</sup> mice at levels similar to WT (Fig. 7A), indicating that this deletion has no effect on  $D_H$  antisense transcription and supporting our reverse transcription-PCR data (Fig. 6). In

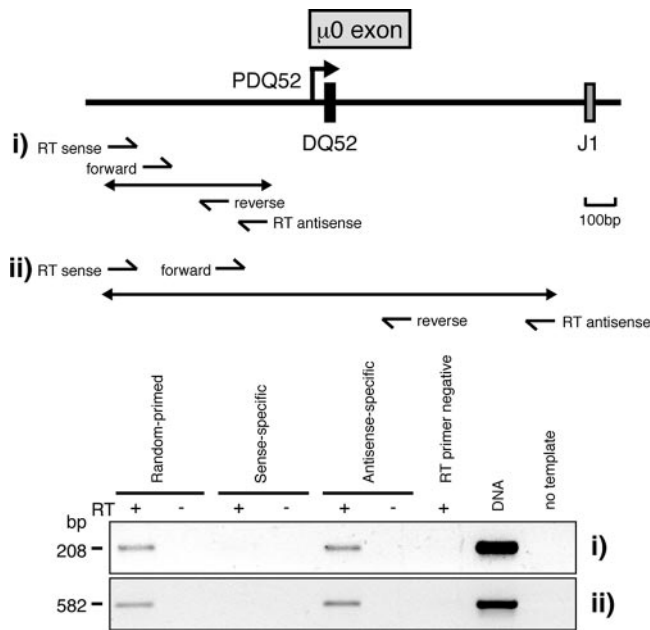


FIG. 6. Analysis of transcription surrounding PDQ52 in *Igh* WT *Rag1*<sup>-/-</sup> mice. Reverse transcription sense and antisense primers were designed in regions 5' and 3' of PDQ52. Nested primers were then used in PCR. Sense transcripts corresponding to  $\mu_0$  were not detected due to placement of the 5' PCR primer upstream of the  $\mu_0$  transcription start site.

striking contrast, the additional absence of  $E_\mu$  caused a dramatic reduction in antisense transcription over both DFL and DSP gene segments (Fig. 7A and B). These data indicate that  $D_H$  antisense transcription is regulated, either directly or indirectly, by  $E_\mu$ , which also regulates D-to-J recombination. In contrast, deletion of  $E_\mu$  did not inhibit  $V_H$  antisense transcription, demonstrating that this process is not regulated by  $E_\mu$  and correlating with the lack of effect of  $E_\mu$  on V-to-DJ recombination (Fig. 7B).

**$D_H$  antisense transcription initiates either within or immediately upstream of the  $E_\mu$  core element.** As we have previously shown that antisense transcription does not occur in the region immediately downstream of  $E_\mu$  (8), we reasoned that the promoter of  $D_H$  antisense transcription was located within  $E_\mu$  or its immediate upstream flanking sequences and thus sought to map transcription further and identify putative promoters in the region between DQ52 and  $E_\mu$ . Bioinformatic analyses using Genomatix Promoter Inspector (10) did not identify any canonical promoter elements. We attempted strand-specific reverse transcription-PCR across this interval using RNA from *Igh*-WT *Rag*-deficient mice. However, this proved impossible due to detection of the high-level  $\mu_0$  sense transcription in the antisense-specific and primer-negative controls due to endogenous priming in the reverse transcription step (not shown). We considered the possibility that  $\mu_0$  primary transcription, and hence endogenous priming, might be significantly reduced in the PDQ52<sup>-/-</sup> *Rag*-deficient mice and that these mice could thereby be used to map the antisense transcription within this region. We have previously shown that levels of mature, spliced  $\mu_0$  mRNA are little changed when PDQ52 is deleted (2) but had not assessed  $\mu_0$  primary transcription in these mice. Semi-

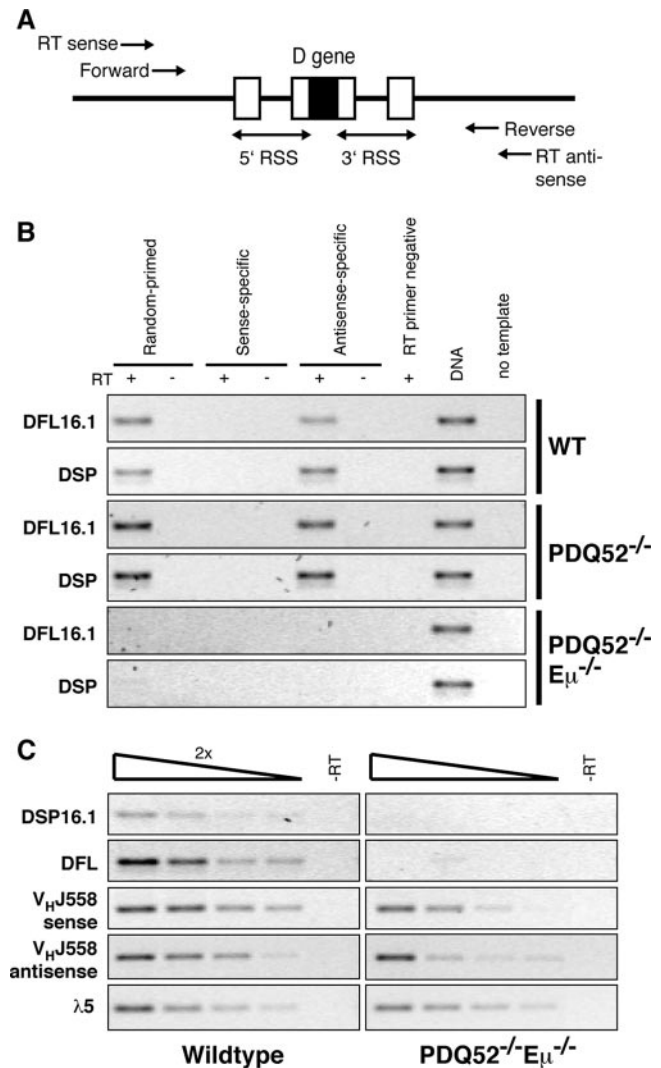


FIG. 7. Reverse transcription-PCR analysis of D and V region germ line transcription in *Igh* WT, PDQ52<sup>-/-</sup>, and PDQ52<sup>-/-</sup> $E_\mu$ <sup>-/-</sup> *Rag1*<sup>-/-</sup> mice. (A) Design of the  $D_H$  gene germ line transcription reverse transcription-PCR assay. (B)  $D_H$  gene strand-specific reverse transcription-PCR of total RNA from B220<sup>+</sup> BM B lymphocytes from *Igh* WT, PDQ52<sup>-/-</sup>, and PDQ52<sup>-/-</sup> $E_\mu$ <sup>-/-</sup> *Rag1*<sup>-/-</sup> mice. (C) Semi-quantitative reverse transcription-PCR of  $D_H$  and  $V_H$  ( $V_HJ558$ ) germ line transcription in WT and PDQ52<sup>-/-</sup> $E_\mu$ <sup>-/-</sup> *Rag1*<sup>-/-</sup> mice.  $\lambda 5$  was used as a loading control.

quantitative reverse transcription-PCR using primers in the  $\mu_0$  intron demonstrated that  $\mu_0$  primary transcription is six- to eightfold reduced when PDQ52 is deleted (data not shown).

As it seemed likely that the antisense transcription was initiating either within or immediately upstream of  $E_\mu$ , we analyzed transcription between J4 and the 222-bp  $E_\mu$  core (22) in PDQ52<sup>-/-</sup> mice. We did strand-specific reverse transcription-PCR using reverse transcription primers located immediately 3' of J4 (antisense specific) and at the 3' margin of the  $E_\mu$  core (sense specific), followed by PCR using three sets of primers in the intervening region (Fig. 8). Antisense-specific products were amplified for the two 5' regions but not the 3' region spanning the  $E_\mu$  core, demonstrating that transcription ini-

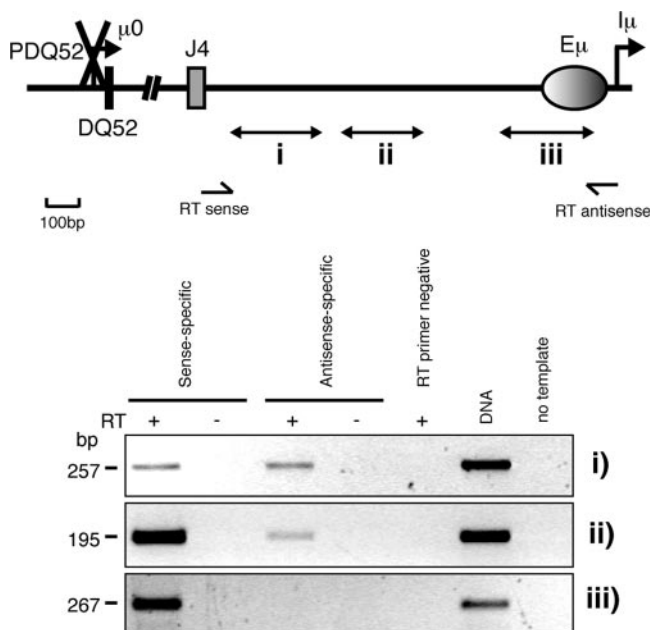


FIG. 8. Mapping of an antisense transcriptional start site to the 5' margin of the  $E_{\mu}$  core. Reverse transcription primers were designed immediately 3' of J4 and at the 3' boundary of the  $E_{\mu}$  core to detect antisense and sense transcription, respectively, across this interval. Three sets of PCR primers in the intervening region were then used to map transcription across this region. Above lanes, with (+) or without (-) reverse transcriptase (RT). DNA, genomic DNA positive control.

tiates either within the  $E_{\mu}$  core or in the 235-bp region immediately upstream.

DISCUSSION

We report the discovery of antisense intergenic transcription throughout the  $D_H$  and  $J_H$  regions of the mouse *Igh* locus in pro-B cells and propose that this process remodels the  $D_H$  cluster for  $D_H$ -to- $J_H$  recombination. In support of this model, we show that D antisense transcription is activated before  $D_H$ -to- $J_H$  recombination and is regulated by the intronic enhancer  $E_{\mu}$ .  $E_{\mu}$  was recently demonstrated to regulate V(D)J recombination of the *Igh* locus at the earliest  $D_H$ -to- $J_H$  recombination step (2). Taken together, these data suggest that  $E_{\mu}$  controls  $D_H$ -to- $J_H$  recombination by activating this form of germ line *Igh* transcription and that the processivity of this transcription renders the D region accessible for  $D_H$ -to- $J_H$  recombination. To our knowledge, this is the first report for an endogenous locus of a regulatory element ( $E_{\mu}$ ) regulating both intergenic transcription and a process that requires chromatin accessibility of the transcribed region, in this case,  $D_H$ -to- $J_H$  recombination. This model is supported by a recent report that intergenic transcription regulates  $J\alpha$  gene recombination in the TCR $\alpha$  locus (1).

In contrast to transcription over the D region, we show that deletion of  $E_{\mu}$  has no effect on  $V_H$  antisense transcription, suggesting that accessibility of the  $V_H$  region is not regulated by  $E_{\mu}$ , in agreement with  $E_{\mu}$ 's not having a major role in  $V_H$ -to- $DJ_H$  recombination (2, 49). Furthermore, we show that  $D_H$  antisense transcripts initiate on germ line alleles and that

$D_H$  and  $V_H$  antisense transcripts are rarely associated on individual alleles. Thus, we demonstrate a stepwise progression of antisense intergenic transcription, first over the DJ region, under the control of  $E_{\mu}$ , then over the V region, under the control of a separate, unknown, regulatory element. In both cases, transcription precedes the corresponding V(D)J recombination event. This pattern is strikingly similar to the observed stepwise progression of active histone marks during *Igh* V(D)J recombination (15). Our results raise an important question: what regulates V region intergenic transcription? We have ruled out the P/Q52 promoter/enhancer, since V antisense transcription is normal in P/Q52 knockout mice. Interestingly, a novel pro-B cell-specific hypersensitive site has recently been identified 5' of the V region, although its function is not yet known (48).

We have discovered that a major transcription start site for D region antisense transcription lies either within the  $E_{\mu}$  core or in the upstream J-proximal 235-bp region including the 5' MAR (Fig. 8). Since the enhancer core and upstream region are both deleted in the  $E_{\mu}$  knockout mice we analyzed here, we are currently unable to distinguish between a putative antisense promoter and the known enhancer functions of the  $E_{\mu}$  core. However, we have compared these mice with mice that lack the  $E_{\mu}$  core but have the upstream region intact (49), and both have a similar defect in *Igh* D-to-J recombination (2). This suggests a dominant role for the  $E_{\mu}$  core in this process, either as a bona fide enhancer, an as-yet-unclassified promoter, or both.

We propose that antisense intergenic transcription over  $D_H$  facilitates the establishment of an active chromatin domain for  $D_H$ -to- $J_H$  recombination, either by histone exchange or recruitment of chromatin modifiers. Our model is supported by several observations. First, intergenic transcription is concomitant with a decrease in repressive histone marks, including dimethyl histone H3K9, and an increase in active histone marks, including H3 acetylation, and chromatin-remodeling enzymes over the  $DJ_H$  region prior to  $D_H$ -to- $J_H$  recombination (15, 37, 43). Histone acetylation is highest over the J region but is also widespread throughout the D region (15). This is consistent with histone acetylation's being propagated by intergenic transcription initiating near  $E_{\mu}$  and decreasing with increasing distance from the start site. However, it is not yet clear whether there is a continuous antisense transcript starting close to  $E_{\mu}$  or multiple smaller transcripts initiating throughout the D locus. Since this is a large region (60 kb), it is also possible that  $E_{\mu}$  controls transcription in cooperation with more than one antisense promoter. This model is in agreement with a recent suggestion that the region encompassing DQ52 and the four J genes and  $E_{\mu}$  forms a separate chromatin domain from the rest of the D region (37).

Conversely, this study provides substantial evidence opposing a role for antisense transcription in generation of double-stranded RNA (dsRNA) and heterochromatin formation in the *Igh* locus. Strikingly, the J region, which displays the highest histone acetylation before D-to-J recombination, forms part of the transcription overlap between the  $\mu_0$  sense transcript and antisense transcription originating near  $E_{\mu}$ , suggesting that the transcription units are not antagonistic. Indeed, they are coordinately upregulated by  $E_{\mu}$ . Furthermore, over DQ52, the single D gene that expresses sense transcripts,  $D_H$

antisense and  $\mu_0$  (sense) are cotranscribed on the same allele, yet DQ52 is rather more acetylated than the rest of the D genes (15, 43) and is preferentially used in early D-to-J recombination (6). Additionally, our finding that there is no sense germ line transcription in the remainder of the  $D_H$  region indicates that there is no possibility for dsRNA formation. Intergenic transcription has recently been shown to be required for V(D)J recombination at the TCR $\alpha$  locus, but in this case, it originates from the sense strand (1). This suggests that the strand origin is not important, which supports our model that the processing activity is the key function of this transcription.

Why is a large-scale chromatin remodeling process necessary? The  $D_H$  genes are small (11 to 16 bp) relative to the large intergenic sequences between them (4 kb). However, relocation of the *Igh* locus from the nuclear periphery to the interior precedes D-to-J recombination and requires chromatin unfolding (32). Furthermore, *Igh* must be made accessible to the large RAG recombinase complex. It is unlikely that either could be achieved through remodeling of the genes alone. Instead, intergenic transcription may alter the chromatin structure throughout the large DJ region (60 kb) in a similar manner to other large developmentally regulated loci (40), which undergo transcription-dependent (39, 44), higher-order chromatin remodeling and looping out of their chromosome territories (13, 62). Furthermore, we speculate that  $E_\mu$  may promote nuclear relocation by recruiting the D region to a transcription factory in the nuclear interior to facilitate intergenic transcription, in a similar manner to the  $\beta$ -globin locus control region (50).

Recombination of most antigen receptor loci (e.g., TCR $\alpha$ , TCR $\beta$ , and Igk loci) requires the cooperative activity of germ line promoters and enhancers and is characterized by transcription from germ line promoters (34). Of particular interest are the promoters upstream of each D $\beta$  gene cluster in the TCR $\beta$  locus (PD $\beta$ 1 and PD $\beta$ 2) (56) and both upstream of and within the TCR $\alpha$  J cluster (27), which are required for efficient D $\beta$ -J $\beta$  (63, 64) and V $\alpha$ -J $\alpha$  (27) joining, respectively. The transcribed regions are associated with active histone marks such as acetylation (41, 64). These promoters require the presence of their respective intronic enhancer elements ( $E_\beta$  and  $E_\alpha$ ) for transcriptional activity (34). We have recently shown that  $E_\beta$  has two distinct roles prior to V(D)J recombination of the TCR $\beta$  locus: an intrinsic function that directs general chromatin opening over most of the D $\beta$ J $\beta$  cluster and a cooperative function that facilitates the assembly of a promoter/enhancer holocomplex with PD $\beta$ 1 (46). Here we show that the  $D_H$  cluster differs from this and other antigen receptor loci in that transcription is undetectable from most  $D_H$  germ line promoters. This raises the possibility that interaction between D promoters and  $E_\mu$  may not occur and may not be necessary for  $D_H$ -to- $J_H$  recombination. Further, deletion of the only promoter from which germ line transcription was detected, DQ52, had no effect on antisense intergenic transcription, shown here, or D-to-J recombination (2), although in this case arguably a promoter-enhancer interaction might not be necessary due to proximity of DQ52 to  $E_\mu$ . Thus, it is possible that  $E_\mu$  enhancer-driven antisense intergenic transcription may be the major force driving accessibility over the  $D_H$  region prior to DJ recombination. However, absence of transcription does not pre-

clude interaction of the germ line promoters with  $E_\mu$ , and such an interaction may occur before recombination and expression of the  $D_\mu$  transcript. It will be interesting to distinguish between these possibilities by direct analysis of the interaction of these elements.

In summary, we have discovered that, in addition to the  $V_H$  region, antisense intergenic transcription occurs throughout the *Igh* D region and is thus a widespread process during V(D)J recombination.  $D_H$  antisense intergenic transcription precedes  $D_H$ -to- $J_H$  recombination and initiates near to and is regulated by  $E_\mu$ . Since  $E_\mu$  also regulates  $D_H$ -to- $J_H$  recombination, antisense intergenic transcription may provide a long-distance, processive mechanism by which  $E_\mu$  is able to regulate accessibility across the  $D_H$  region.

#### ACKNOWLEDGMENTS

We thank Peter Fraser and Lyubomira Chakalova for critical review of the manuscript and Geoff Morgan for help with FACS.

D.B., A.W., and A.E.C. were supported by the Biotechnology and Biological Sciences Research Council including grant number BB/C508769/1 (D.B.), and R.A. and E.M.O. were supported by grants from the National Institutes of Health (P01 HL68744 and CA100905, E.M.O.; T32 CA09385, R.A.) and a Cancer Center Support grant (P30 CA68485, Vanderbilt-Ingram Cancer Center).

We declare that we have no financial interests that pose a conflict of interest with regard to this article.

#### REFERENCES

1. Abarrategui, I., and M. S. Krangel. 2006. Regulation of T cell receptor-alpha gene recombination by transcription. *Nat. Immunol.* 7:1109–1115.
2. Afshar, R., S. Pierce, D. J. Bolland, A. Corcoran, and E. M. Oltz. 2006. Regulation of IgH gene assembly: role of the intronic enhancer and 5'DQ52 region in targeting DHJH recombination. *J. Immunol.* 176:2439–2447.
3. Alessandrini, A., and S. V. Desiderio. 1991. Coordination of immunoglobulin DJH transcription and D-to-JH rearrangement by promoter-enhancer approximation. *Mol. Cell. Biol.* 11:2096–2107.
4. Allman, D., J. Li, and R. R. Hardy. 1999. Commitment to the B lymphoid lineage occurs before DH-JH recombination. *J. Exp. Med.* 189:735–740.
5. Atkinson, M. J., D. A. Michnick, C. J. Paige, and G. E. Wu. 1991. Ig gene rearrangements on individual alleles of Abelson murine leukemia cell lines from (C57BL/6  $\times$  BALB/c) F1 fetal livers. *J. Immunol.* 146:2805–2812.
6. Bangs, L. A., I. E. Sanz, and J. M. Teale. 1991. Comparison of D, JH, and junctional diversity in the fetal, adult, and aged B cell repertoires. *J. Immunol.* 146:1996–2004.
7. Bernstein, B. E., M. Kamal, K. Lindblad-Toh, S. Bekiranov, D. K. Bailey, D. J. Huebert, S. McMahon, E. K. Karlsson, E. J. Kulbokas III, T. R. Gingeras, S. L. Schreiber, and E. S. Lander. 2005. Genomic maps and comparative analysis of histone modifications in human and mouse. *Cell* 120:169–181.
8. Bolland, D. J., A. L. Wood, C. M. Johnston, S. F. Bunting, G. Morgan, L. Chakalova, P. J. Fraser, and A. E. Corcoran. 2004. Antisense intergenic transcription in V(D)J recombination. *Nat. Immunol.* 5:630–637.
9. Born, W., J. White, J. Kappler, and P. Marrack. 1988. Rearrangement of IgH genes in normal thymocyte development. *J. Immunol.* 140:3228–3232.
10. Cartharius, K., K. Frech, K. Grote, B. Klocke, M. Haltmeier, A. Klingenhoff, M. Frisch, M. Bayerlein, and T. Werner. 2005. MatInspector and beyond: promoter analysis based on transcription factor binding sites. *Bioinformatics* 21:2933–2942.
11. Chakalova, L., D. Carter, and P. Fraser. 2004. RNA fluorescence in situ hybridization tagging and recovery of associated proteins to analyze in vivo chromatin interactions. *Methods Enzymol.* 375:479–493.
12. Chakalova, L., E. Debrand, J. A. Mitchell, C. S. Osborne, and P. Fraser. 2005. Replication and transcription: shaping the landscape of the genome. *Nat. Rev. Genet.* 6:669–677.
13. Chambeyron, S., N. R. Da Silva, K. A. Lawson, and W. A. Bickmore. 2005. Nuclear re-organisation of the Hoxb complex during mouse embryonic development. *Development* 132:2215–2223.
14. Cho, H., G. Orphanides, X. Sun, X. J. Yang, V. Ogryzko, E. Lees, Y. Nakatani, and D. Reinberg. 1998. A human RNA polymerase II complex containing factors that modify chromatin structure. *Mol. Cell. Biol.* 18:5355–5363.
15. Chodhury, D., and R. Sen. 2001. Stepwise activation of the immunoglobulin mu heavy chain gene locus. *EMBO J.* 20:6394–6403.
16. Corcoran, A. E. 2005. Immunoglobulin locus silencing and allelic exclusion. *Semin. Immunol.* 17:141–154.

17. **Corcoran, A. E., A. Riddell, D. Krooshoop, and A. R. Venkitaraman.** 1998. Impaired immunoglobulin gene rearrangement in mice lacking the IL-7 receptor. *Nature* **391**:904–907.
18. **Cumano, A., and C. J. Paige.** 1992. Enrichment and characterization of uncommitted B-cell precursors from fetal liver at day 12 of gestation. *EMBO J.* **11**:593–601.
19. **Delassus, S., and A. Cumano.** 1996. Circulation of hematopoietic progenitors in the mouse embryo. *Immunity* **4**:97–106.
20. **Delassus, S., S. Darche, P. Kourilsky, and A. Cumano.** 1998. Ontogeny of the heavy chain immunoglobulin repertoire in fetal liver and bone marrow. *J. Immunol.* **160**:3274–3280.
21. **Drewell, R. A., E. Bae, J. Burr, and E. B. Lewis.** 2002. Transcription defines the embryonic domains of cis-regulatory activity at the *Drosophila* bithorax complex. *Proc. Natl. Acad. Sci. USA* **99**:16853–16858.
22. **Ernst, P., and S. T. Smale.** 1995. Combinatorial regulation of transcription II: the immunoglobulin mu heavy chain gene. *Immunity* **2**:427–438.
23. **Fuxa, M., J. Skok, A. Souabni, G. Salvagiotto, E. Roldan, and M. Busslinger.** 2004. Pax5 induces V-to-DJ rearrangements and locus contraction of the immunoglobulin heavy-chain gene. *Genes Dev.* **18**:411–422.
24. **Gribnau, J., E. de Boer, T. Trimborn, M. Wijgerde, E. Milot, F. Grosveld, and P. Fraser.** 1998. Chromatin interaction mechanism of transcriptional control in vivo. *EMBO J.* **17**:6020–6027.
25. **Gribnau, J., K. Diderich, S. Pruzina, R. Calzolari, and P. Fraser.** 2000. Intergenic transcription and developmental remodeling of chromatin subdomains in the human beta-globin locus. *Mol. Cell* **5**:377–386.
26. **Hardy, R. R., Y. S. Li, D. Allman, M. Asano, M. Gui, and K. Hayakawa.** 2000. B-cell commitment, development and selection. *Immunol. Rev.* **175**:23–32.
27. **Hawwari, A., C. Bock, and M. S. Krangel.** 2005. Regulation of T cell receptor alpha gene assembly by a complex hierarchy of germline J $\alpha$  promoters. *Nat. Immunol.* **6**:481–489.
28. **Hesslein, D. G., and D. G. Schatz.** 2001. Factors and forces controlling V(D)J recombination. *Adv. Immunol.* **78**:169–232.
29. **Johnson, K., C. Angelin-Duclos, S. Park, and K. L. Calame.** 2003. Changes in histone acetylation are associated with differences in accessibility of V(H) gene segments to V-DJ recombination during B-cell ontogeny and development. *Mol. Cell. Biol.* **23**:2438–2450.
30. **Johnson, K., D. L. Pflugh, D. Yu, D. G. Hesslein, K. I. Lin, A. L. Bothwell, A. Thomas-Tikhonenko, D. G. Schatz, and K. Calame.** 2004. B cell-specific loss of histone 3 lysine 9 methylation in the V(H) locus depends on Pax5. *Nat. Immunol.* **5**:853–861.
31. **Johnston, C. M., A. L. Wood, D. J. Bolland, and A. E. Corcoran.** 2006. Complete sequence assembly and characterization of the C57BL/6 mouse Ig heavy chain V region. *J. Immunol.* **176**:4221–4234.
32. **Kosak, S. T., J. A. Skok, K. L. Medina, R. Riblet, M. M. Le Beau, A. G. Fisher, and H. Singh.** 2002. Subnuclear compartmentalization of immunoglobulin loci during lymphocyte development. *Science* **296**:158–162.
33. **Kottmann, A. H., B. Zevnik, M. Welte, P. J. Nielsen, and G. Kohler.** 1994. A second promoter and enhancer element within the immunoglobulin heavy chain locus. *Eur. J. Immunol.* **24**:817–821.
34. **Krangel, M. S.** 2003. Gene segment selection in V(D)J recombination: accessibility and beyond. *Nat. Immunol.* **4**:624–630.
35. **Lennon, G. G., and R. P. Perry.** 1985. C mu-containing transcripts initiate heterogeneously within the IgH enhancer region and contain a novel 5'-nontranslatable exon. *Nature* **318**:475–478.
36. **Lennon, G. G., and R. P. Perry.** 1990. The temporal order of appearance of transcripts from unrearranged and rearranged Ig genes in murine fetal liver. *J. Immunol.* **144**:1983–1987.
37. **Maes, J., S. Chappaz, P. Cavelier, L. O'Neill, B. Turner, F. Rougeon, and M. Goodhardt.** 2006. Activation of V(D)J recombination at the IgH chain JH locus occurs within a 6-kilobase chromatin domain and is associated with nucleosomal remodeling. *J. Immunol.* **176**:5409–5417.
38. **Maes, J., L. P. O'Neill, P. Cavelier, B. M. Turner, F. Rougeon, and M. Goodhardt.** 2001. Chromatin remodeling at the Ig loci prior to V(D)J recombination. *J. Immunol.* **167**:866–874.
39. **Mahy, N. L., P. E. Perry, and W. A. Bickmore.** 2002. Gene density and transcription influence the localization of chromatin outside of chromosome territories detectable by FISH. *J. Cell Biol.* **159**:753–763.
40. **Mastermak, K., N. Peyraud, M. Krawczyk, E. Barras, and W. Reith.** 2003. Chromatin remodeling and extragenic transcription at the MHC class II locus control region. *Nat. Immunol.* **4**:132–137.
41. **Mauvieux, L., I. Villey, and J. P. de Villartay.** 2003. TEA regulates local TCR-Jalpa accessibility through histone acetylation. *Eur. J. Immunol.* **33**:2216–2222.
42. **Mito, Y., J. G. Henikoff, and S. Henikoff.** 2005. Genome-scale profiling of histone H3.3 replacement patterns. *Nat. Genet.* **37**:1090–1097.
43. **Morshead, K. B., D. N. Ciccone, S. D. Taverna, C. D. Allis, and M. A. Oettinger.** 2003. Antigen receptor loci poised for V(D)J rearrangement are broadly associated with BRG1 and flanked by peaks of histone H3 dimethylated at lysine 4. *Proc. Natl. Acad. Sci. USA* **100**:11577–11582.
44. **Muller, W. G., D. Walker, G. L. Hager, and J. G. McNally.** 2001. Large-scale chromatin decondensation and recondensation regulated by transcription from a natural promoter. *J. Cell Biol.* **154**:33–48.
45. **Nguyen, Q. T., N. Doyen, M. F. d'Andon, and F. Rougeon.** 1991. Demonstration of a divergent transcript from the bidirectional heavy chain immunoglobulin promoter VH441 in B-cells. *Nucleic Acids Res.* **19**:5339–5344.
46. **Oestreich, K. J., R. M. Cobb, S. Pierce, J. Chen, P. Ferrier, and E. M. Oltz.** 2006. Regulation of TCRbeta gene assembly by a promoter/enhancer holocomplex. *Immunity* **24**:381–391.
47. **Orphanides, G., and D. Reinberg.** 2000. RNA polymerase II elongation through chromatin. *Nature* **407**:471–475.
48. **Pawlitzky, I., C. V. Angeles, A. M. Siegel, M. L. Stanton, R. Riblet, and P. H. Brodeur.** 2006. Identification of a candidate regulatory element within the 5' flanking region of the mouse IgH locus defined by pro-B cell-specific hypersensitivity associated with binding of PU.1, Pax5, and E2A. *J. Immunol.* **176**:6839–6851.
49. **Perlot, T., F. W. Alt, C. H. Bassing, H. Suh, and E. Pinaud.** 2005. Elucidation of IgH intronic enhancer functions via germ-line deletion. *Proc. Natl. Acad. Sci. USA* **102**:14362–14367.
50. **Ragoczy, T., M. A. Bender, A. Telling, R. Byron, and M. Groudine.** 2006. The locus control region is required for association of the murine beta-globin locus with engaged transcription factories during erythroid maturation. *Genes Dev.* **20**:1447–1457.
51. **Reth, M. G., and F. W. Alt.** 1984. Novel immunoglobulin heavy chains are produced from DJH gene segment rearrangements in lymphoid cells. *Nature* **312**:418–423.
52. **Sakai, E., A. Bottaro, L. Davidson, B. P. Sleckman, and F. W. Alt.** 1999. Recombination and transcription of the endogenous Ig heavy chain locus is effected by the Ig heavy chain intronic enhancer core region in the absence of the matrix attachment regions. *Proc. Natl. Acad. Sci. USA* **96**:1526–1531.
53. **Sayegh, C., S. Jhunjhunwala, R. Riblet, and C. Murte.** 2005. Visualization of looping involving the immunoglobulin heavy-chain locus in developing B cells. *Genes Dev.* **19**:322–327.
54. **Schwartz, B. E., and K. Ahmad.** 2005. Transcriptional activation triggers deposition and removal of the histone variant H3.3. *Genes Dev.* **19**:804–814.
55. **Serwe, M., and F. Sablitzky.** 1993. V(D)J recombination in B cells is impaired but not blocked by targeted deletion of the immunoglobulin heavy chain intron enhancer. *EMBO J.* **12**:2321–2327.
56. **Sikes, M. L., R. J. Gomez, J. Song, and E. M. Oltz.** 1998. A developmental stage-specific promoter directs germline transcription of D beta J beta gene segments in precursor T lymphocytes. *J. Immunol.* **161**:1399–1405.
57. **Spanopoulou, E., C. A. Roman, L. M. Corcoran, M. S. Schlissel, D. P. Silver, D. Nemaze, M. C. Nussenzweig, S. A. Shinton, R. R. Hardy, and D. Baltimore.** 1994. Functional immunoglobulin transgenes guide ordered B-cell differentiation in Rag-1-deficient mice. *Genes Dev.* **8**:1030–1042.
58. **Stanhope-Baker, P., K. M. Hudson, A. L. Shaffer, A. Constantinescu, and M. S. Schlissel.** 1996. Cell type-specific chromatin structure determines the targeting of V(D)J recombinase activity in vitro. *Cell* **85**:887–897.
59. **Su, I. H., A. Basavaraj, A. N. Krutchinsky, O. Hobert, A. Ullrich, B. T. Chait, and A. Tarakhovskiy.** 2003. Ezh2 controls B cell development through histone H3 methylation and Igh rearrangement. *Nat. Immunol.* **4**:124–131.
60. **Thompson, A., E. Timmers, R. K. Schuurman, and R. W. Hendriks.** 1995. Immunoglobulin heavy chain germ-line JH-C mu transcription in human precursor B lymphocytes initiates in a unique region upstream of DQ52. *Eur. J. Immunol.* **25**:257–261.
61. **Trimborn, T., J. Gribnau, F. Grosveld, and P. Fraser.** 1999. Mechanisms of developmental control of transcription in the murine alpha- and beta-globin loci. *Genes Dev.* **13**:112–124.
62. **Volpi, E. V., E. Chevret, T. Jones, R. Vatcheva, J. Williamson, S. Beck, R. D. Campbell, M. Goldsworthy, S. H. Powis, J. Ragoussis, J. Trowsdale, and D. Sheer.** 2000. Large-scale chromatin organization of the major histocompatibility complex and other regions of human chromosome 6 and its response to interferon in interphase nuclei. *J. Cell Sci.* **113**:1565–1576.
63. **Whitehurst, C. E., S. Chattopadhyay, and J. Chen.** 1999. Control of V(D)J recombinational accessibility of the D beta 1 gene segment at the TCR beta locus by a germline promoter. *Immunity* **10**:313–322.
64. **Whitehurst, C. E., M. S. Schlissel, and J. Chen.** 2000. Deletion of germline promoter PD beta 1 from the TCR beta locus causes hypermethylation that impairs D beta 1 recombination by multiple mechanisms. *Immunity* **13**:703–714.
65. **Wilson, C. J., D. M. Chao, A. N. Imbalzano, G. R. Schnitzler, R. E. Kingston, and R. A. Young.** 1996. RNA polymerase II holoenzyme contains SWI/SNF regulators involved in chromatin remodeling. *Cell* **84**:235–244.
66. **Wittschieben, B. O., G. Otero, T. de Bizemont, J. Fellows, H. Erdjument-Bromage, R. Ohba, Y. Li, C. D. Allis, P. Tempst, and J. Q. Svejstrup.** 1999. A novel histone acetyltransferase is an integral subunit of elongating RNA polymerase II holoenzyme. *Mol. Cell* **4**:123–128.
67. **Yancopoulos, G. D., and F. W. Alt.** 1985. Developmentally controlled and tissue-specific expression of unrearranged VH gene segments. *Cell* **40**:271–281.
68. **Ye, J.** 2004. The immunoglobulin IGHD gene locus in C57BL/6 mice. *Immunogenetics* **56**:399–404.